CALCULATION OF TEMPERATURE DISTRIBUTION OF AIR-COOLED THREE-PHASE DRY TRANSFORMER

TÍNH TOÁN PHÂN BỐ NHIỆT MÁY BIẾN ÁP KHÔ BA PHA LÀM MÁT BẰNG KHÔNG KHÍ

Bao Doan Thanh*

Quy Nhon University

*Corresponding author: doanthanhbao@qnu.edu.vn

(Received: September 15, 2021; Accepted: November 07, 2022)

Abstract - We want to make longer the life of the transformer and we need to effectively solve cooling and heat transfer problems. A mathematical model in this paper is developed and set up to calculate the heat for a 560kVA power transformer. This paper is performed by two experimental methods and Computational Fluid Dynamics. Thermal analysis and calculation are performed on various points on the coil or barrel surface. Correspondingly, the temperature distribution is calculated for the different working modes of the transformer in the case of no-load and rated and short-circuit. Description of heat transfer, temperature flows in an explosion-proof enclosure. In addition, the hottest spots on the coil or sheath surface are found. From the results, it is open to study thermal calculation method models for different electrical equipments and machines.

Key words - Transformer; Short-circuit; Temperature; Computational Fluid Dynamics; Cooling.

Tóm tắt – Để tuổi thọ của máy biến áp được nâng cao, chúng ta cần giải quyết hiệu quả các vấn đề làm mát và truyền nhiệt. Bài báo này thiết lập một mô hình toán học để tính nhiệt cho máy biến áp công suất 560kVA. Bài báo này được thực hiện bằng hai phương pháp thực nghiệm và động lực học chất lưu. Phân tích và tính toán nhiệt trên nhiều điểm khác nhau trên bề mặt cuộn dây hoặc vỏ thùng. Đồng thời, phân bố nhiệt độ được tính toán các chế độ làm việc khác nhau của máy biến áp trong trường hợp không tải, định mức và ngắn mạch. Mô tả truyền nhiệt, dòng nhiệt độ trong vỏ bọc chống cháy nổ. Bên cạnh đó, tìm ra các điểm nóng nhất trên bề mặt cuộn dây hoặc vỏ thùng. Từ kết quả này, mở ra hướng nghiên cứu, tính toán mô hình nhiệt cho các thiết bị điện và máy điện khác.

Từ khóa – Máy biến áp; ngắn mạch; nhiệt độ, động lực học chất lưu; làm mát.

1. Introduction

When operating transformers, we also pay attention to the electrical parameters, the temperature parameters on the steel core and windings are very important. If it is effectively solved the cooling problem, the transformer's life will be greatly increased. The process of temperature transferring and cooling of dry transformers is very complex and sometimes more difficult than that of oil transformers. Especially, the dry pressure machine is naturally cooled by air, it is used in underground mines, where there is a danger of explosion of methane gas and/or coal dust. The transformer is pre-designed in an explosion-proof enclosure, with different internal and external atmospheres, it works under strict operating conditions on cooling [1-4]. Therefore, it is required to find mathematical models/processes to calculate the temperature distribution inside and outside the enclosure; Accurate determination of the hottest spot in the core and windings is essential for air-cooled dry transformers [5-7].

The authors [8, 9] used the Finite Element Method (FEM) to calculate the electromagnetic force when a short circuit occurs, the temperature difference between the winding and the epoxy layer and the temperature distribution of the non-copper in the epoxy layer. Studying heat calculation using formulas to calculate average values and not showing the location with the highest temperature in core or windings.

The authors [10] provide a mathematical model of the dry transformer heat distribution, the finite difference method model is compared with the experimental method with the same results. Many authors also study the temperature distribssution in dry transformers by the finite element method [11]. In order to solve temperature, transfer problems and simulate heat distribution, different research methods are used, which are: analytical or "semi-analytic" methods such as equivalent alternative thermal circuits and other methods. Numerical methods to build thermal field models are used [12, 13].

The authors [14] have proposed a mathematical study that is the temperature distribution field model, and it is the numerical solver to solve the differential equations of the thermal field of the transformer built from the model physics. The transformer temperature field model is used with two numerical solutions: FEM and Computational Fluid Dynamics (CFD).

In the study [15], Wang Ning used the COMSOL Multiphysics method to simulate the 3D temperature distribution of dry transformers, verifying the results between simulation and experimental measurements, thereby proving the accuracy of the model. The results show that the higher temperature is concentrated in the upper region of the coils, phase B has a higher temperature than phase A and phase C.

The authors [16] in the study compared the method using the equivalent alternative thermal circuit model (LPTN) and the FEM method. Research has shown that the application of the LPTN model is more feasible. Although, the temperature calculation results are quite different. At the same time, the author's research shows that the hottest temperature is concentrated in the middle of the winding. The hottest temperature of high voltage (HV) winding is 60.89°C and low voltage (LV) winding is 73.83°C.

The authors [17] performed the 3D temperature distribution simulation of amorphous dry transformer SCBH15-600/10. Simulation and experimental results have a 10% error when the same capacity, the amorphous machine is lower the temperature rise than the silicon core transformer. In conclusion, the hottest point is in the B phase LV winding.

With the above comments, we realize there are many research works that have used different methods to calculate and analyze the temperature in dry transformers. However, the thermal research methods mainly only calculate the electromagnetic parameters, but it does not include the influence of the parameters of epoxy materials, does not compare the turbulent temperature regions, and do not consider the temperature, when the transformer is working in no-load, rated and short-circuit.

In our paper, the temperature distribution for the transformer is calculated, we have developed a mathematical model derived from the chaotic kinetic energy model and the radiant temperature transfer inside and outside the tank. Analyzing and calculating heat transfer, and temperature rise of dry air cooled transformer using this mathematical model. The study conducts heat calculation by experimental model and numerical simulation model CFD in case of transformer working at no-load, rated load and short circuit. In the end, the hottest spots on the coil or barrel surfaces are found, which is exactly what we asked for in the first place.

2. Building Mathematics Models

The main source of temperature generation is the loss of the core and windings of the transformer. Then, in the steady state, the temperature difference between the heat source and the surrounding environment is determined by the Fourier - Kirchhoff equation. [1,2]:

$$\nabla(k.\nabla t) + q_{\upsilon} = \rho.c.\omega.\nabla t \tag{1}$$

where: k - the thermal conductivity; t- temperature; q_{υ} - the volumetric heat source; ρ – the density; c - the specific heat and ω - the specific heat.

The transformer has a cooling medium inside and outside the case, according to the momentum equation written as: [17]:

$$\nabla.\omega = 0 \tag{2}$$

$$\rho\omega.\nabla\omega = F - \nabla p + \mu\nabla^2\omega \tag{3}$$

where: F - the body force vector; p - the pressure; μ - the dynamic viscosity.

The motion of the internal and external air (inside and outside the transformer tank) was typical buoyancy-driven flow. Therefore, the above equations were supplemented with the relation describing the density variation:

$$\rho = \frac{p_{op}}{\frac{R}{M}(t+273)} \tag{4}$$

where: p_{op} - the operating constant pressure; R - the gas constant; M - the molar mass.

The preliminary shows that relatively high intensity of the turbulent flow occurred in the air flowing through the ducts between the coils, and between the coils and core, and also in the external air flowing around the external walls of the transformers tanks. For this reason, for the turbulence modeling within this investigation, the standard $K(\varepsilon)$ model was employed. The model is based on a solution of the following transport equations for the turbulent kinetic energy and the turbulent dissipation rate [19]:

$$pK\nabla\omega = \nabla\left[\left(\mu + \frac{\mu_t}{\sigma_K}\right)\nabla K\right] + G_K + G_b - \rho_{\varepsilon} - Y_M \tag{5}$$

Hence

$$pK\nabla\omega = \nabla\left[\left(\mu + \frac{\mu_t}{\sigma_{\varepsilon}}\right)\nabla\varepsilon\right] + C_{1\varepsilon}\frac{\varepsilon}{K}(G_K + C_{3\varepsilon}G_b) - C_{2\varepsilon}\rho\frac{\varepsilon^2}{K} \tag{6}$$

where: K - the turbulent kinetic energy; μ_t - the turbulent dynamic viscosity; σ_K - the turbulent Prandtl number for K; ε - the turbulent dissipation rate; σ_{ε} – the turbulent Prandtl number for ε, G_K - the generation of the turbulence kinetic energy due to the mean velocity gradients; G_b - the generation of the turbulence kinetic energy due to buoyancy; Y_M - the contribution of the fluctuating dilatation in compressible turbulence to the overall dissipation rate and finally $C_{1\varepsilon}$, $C_{2\varepsilon}$ and $C_{3\varepsilon}$ – the constants depending on a variant of the $K(\varepsilon)$ [9].

The mathematical model takes into account forms of heat transfer such as heat conduction, convection and thermal radiation. Radiant heat transfer includes (*) internal radiation and (**) external radiation. The internal radiative heat transfer occurred within the transformer tank filled with the cooling air, while the external radiative heat flux was exchanged between the external tank walls and the transformer surroundings [18].

(*) To solve the internal radiant heat transfer, we use the Discrete Ordinate (DO) model. The DO radiation model is written according to the radiation transfer equation (RTE) as follows:

$$\nabla.\big(I(r,s)s\big) + (a+\sigma_S)I(r,s) = a.n^2\frac{\sigma(t+273)^4}{\pi} + \int_0^{4\pi} I(r,s)\Phi(s,s_S)d\Omega \tag{7}$$

where: $I(r,s)$ the radiation intensity, which depends on position r and direction s; r is the position vector; s - the direction vector; a the absorption coefficient; σ_s - the scattering coefficient; n - the refractive index; σ - the Stefan – Boltzmann constant (σ=5.672x10^{-8} Wm^{-2}K^{-4}); t the local temperature; Φ - the phase function; s_s - the scattering direction vector, and Ω - the solid angle.

(**) The radiative heat transfer from the exterior of the transformer tank did not require activating any of the radiation models. The external radiative heat flux was calculated using the temperature difference of the tank wall ($t_{\omega,i}$) and internal walls of the surrounding room ($t_{\omega,\infty}$). The following equation was used to calculate the total energy loss of the transformer tank due to radiation:

$$Q_r = \sum_{i=1}^{n} A_i.\sigma.\varepsilon_{\omega}\left(\left(t_{\omega,i}+273\right)^4 - \left(t_{\omega,\infty}+273\right)^4\right) \tag{8}$$

where: Q_r - the total heat transfer rate due to radiation from the tank wall; A - the cell face area of the considered tank wall; σ - the stefan - Boltzmann constant; ε_{ω} - the

emissivity; $t_{\omega,i}$ - the local temperature of the tank wall; $t_{\omega,\infty}$ - the wall temperature of surrounding room [20, 21].

3. Geometrical model of transformer

Survey model of a dry transformer placed in an explosion-proof enclosure (explosion-proof transformer) with capacity 560kVA – 6/(1.2/0.69)kV, wiring diagram Y/y, ΔP_n = 3500 W and ΔP_0 = 1500 W. The transformer model is drawn with many design drawings, but here only one model is shown in Figure 1.

3.1. Dimensional model of transformer

Figure 1. *Model of a dry transformer was made the epoxy [1]*

The epoxy dry transformer is naturally cooled, to enhance cooling, additional ventilation ducts are arranged, on both sides of the case. The tank and transformer were naturally cooled within only the surrounding air. The cooling pipes were designed to work in the following way: the heat from the internal air is transferred to the external surfaces of the pipes. Then the heat is conducted through the pipe walls, and finally, it is transferred from the internal pipe walls to the external air flowing through the pipes Figure 2.

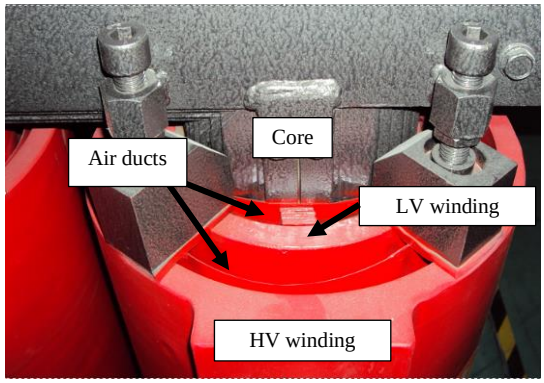

Figure 2. *Top view of the air ducts in the 560 kVA transformer*

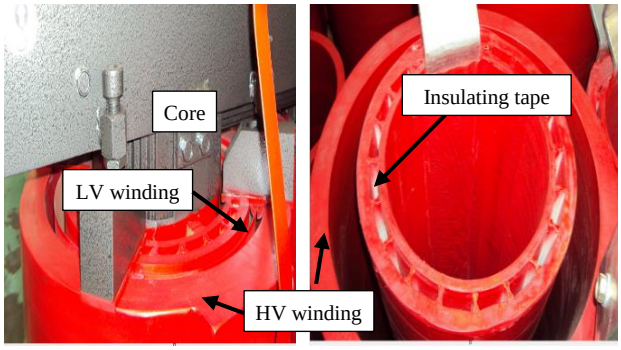

Figure 3. *Geometrical model of winding – core – insulation*

Both primary and secondary windings of the 560 kVA transformer were manufactured using two different techniques. The internal and external parts of the primary coils were resinimmersed coils and consisted of flat wires, wire insulation and interlayer epoxy insulation. Both primary and secondary coils were naturally ventilated by means of the internal air Figure 3.

Epoxy insulating molded resin helps to create an air gap. A total number of turns of the high voltage (HV) winding included 150 turns wound in 3 layers with the overall dimensions of the external part of the primary coil cross-section being 15 mm × 750.0 mm, while those of the internal part were 20 mm × 750.0 mm. Low voltage (LV) winding is wound with copper foil, including 30 turns wound with the overall dimensions of the external part of the primary coils cross-section were 12 mm × 750.0 mm, while those of the internal part were 13 mm × 750.0 mm.

3.2. Material properties for thermal model

Computational modeling is performed at a steady state, the thermal properties of solid materials in Kirchhoff's Fourier equation are thermal conductivity, radiation and emission. The material properties for solids were measured, provided by manufacturers [19] and gathered from the standard literature [1, 2]. The values of the thermal conductivity and the emissivity are defined in Table 1.

Table 1. *Thermal material properties steel and copper*

Transformer elements	Thermal conductivity, $Wm^{-1}K^{-1}$	Emissivity
Copper for wires	385	-
Wire insulating materials	0.2	0.95
Coil interlayer materials	0.13	0.95
Steel sheets for core	40	-
Steel sheets coating	0.44	0.93
Carbon steel for, cooling coil, tank, clampings, screws,	0.35	0.98
Insulating material for locating pads	0.57	0.95
Bakelite for insulation shields	0.23	0.85

4. Procedures for the Experimental measurements

The temperature tests are made by utilizing the rises obtained from the two tests, one with no load loss only, and one with load losses only, i.e. the open- and short-circuit run. The no-load test, at a nominal voltage, was continued until the steady-state conditions were obtained. Then the individual winding temperature rises, Δt_e, were measured. The short-circuit run with a nominal current flowing in one winding and the other winding short-circuited was started immediately following the no-load run, and continued until the steady-state conditions were obtained and the individual winding temperature rises Δt_c were measured.

During the temperature test, the highlight field was monitored by means of five thermocouples mounted within the transformer tank. The sensors measured temperatures on the top surface of the core above each leg, the air between the core and the top wall of the tank, and the air in the duct between a left core leg and the secondary internal coil (points 3÷7 in Figure 4). Moreover, the thermometers captured the temperatures of the air at the inlet and the outlet of the central cooling pipe (points 1–2 in Figure 4).

Additionally, the temperatures of the external surfaces of the transformer tank were also monitored by means of infrared thermography.

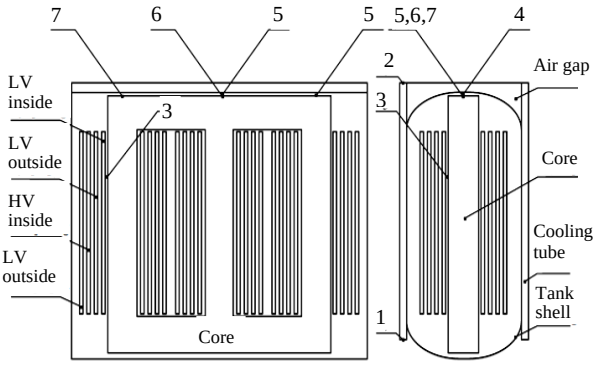

Figure 4. *Schematic layout of the thermocouples and thermometer locations within the transformer station*

5. Simulations model by CFD analysis

All dimensions, electrical specifications, winding construction and material properties are in Section III. It is the input data for CFD analysis. The mathematical model required the solution of the thermal-flow problem including the governing equations, source terms, boundary conditions and material properties. In this study, it is assumed that the winding and the core are like a homogeneous material and there is only one equivalent value for the thermal conductivity in each direction, and the uniform heat source. The model for solving thermal problems by CFD follows [22].

The study used three-dimensional mesh and geometric simulation methods to calculate electromagnetics according to Gambit, using Ansys Fluent and Ansys Maxwell, Ansys workbench whole range of Ansys software Ansys software V.19R1 is copyrighted software installed at Quy Nhon University [22].

The generation of the fine mesh in the transformer geometry was complicated and required a high number of elements. Eventually, for the CFD computations, a mesh with 5 million elements was created. The numerical model with such a large mesh size was solved using parallel processing.

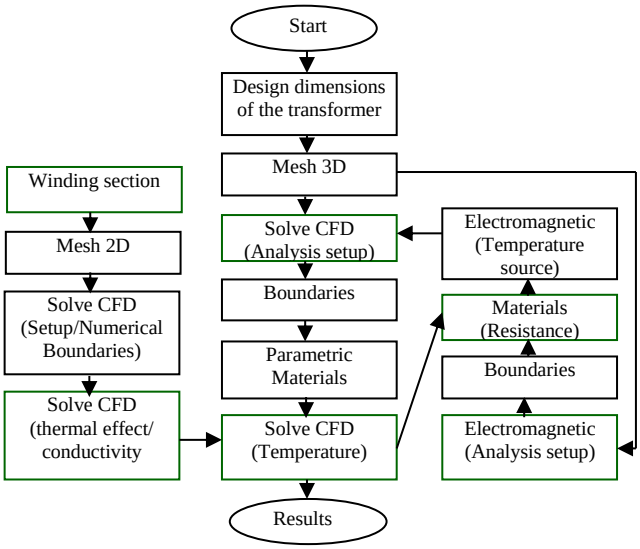

Figure 5. *Coupling scheme for the CFD-electromagnetic solutions*

In successive iterations, the CFD solver generates a new temperature field to update the resistivity and electromagnetic code values, using this information to recalculate the transformer heat loss. The iterations are continued until the error of the number of updates becomes negligible. The combination of heat transfer, fluid flow and electromagnetic problems is schematically described in Figure 5.

6. Comparisons of the Experimental and CFD simulations model

The CFD numerical simulation model shows the results of the temperature distribution corresponding to the flux of the transformer operating in different modes; it shows the temperature at different points in the survey area; it shows the heat at the core sections in Figure 6.

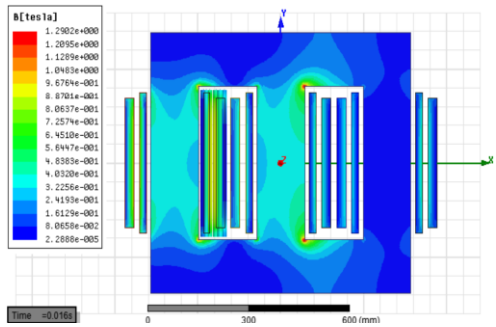

Figure 6. *Temperature distribution (^0C) corresponding to the magnetic flux B(T)*

6.1. No – load

The CFD numerical simulations and Experiments are analyzed at no-load mode. The temperature distribution results are shown in Figure 7 and Figure 8.

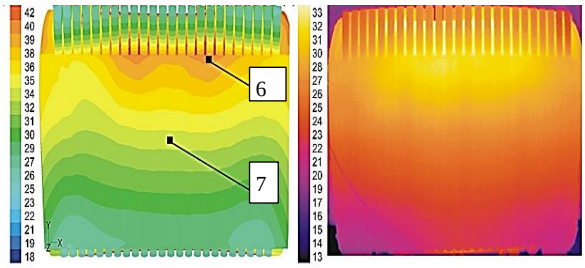

a) *b)*

Figure 7. *Temperature distribution (^0C) of tank shell outside in no load; a) Numerical simulation CFD; b) Experimental measurement*

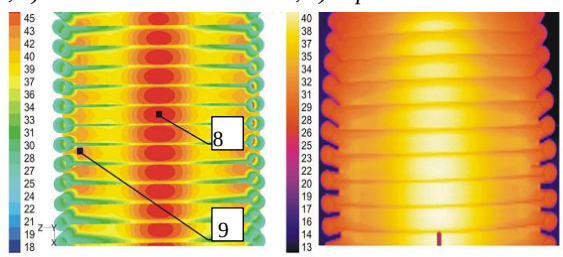

a) *b)*

Figure 8. *Temperature distribution (^0C) top of tank shell outside in no load; a) Numerical simulation CFD b) Experimental measurement*

Discussion of results in No load mode:

At no load, see Figure 6, As a result of these calculations, the heat source for the core was determined in the range of $q_v = 2.1 \div 270$ kWm^{-3}. The average value of a source term

was about $\bar{q}_\vartheta = 101.5$ kW m^{-3}. See Figure 9, Since only the core generated heat, this element had the highest temperature, the temperature at the highest point can be up to 101^{o}C, and large differences along the height of the core can be observed. During both the CFD simulations and the experimental model, the position temperatures inside the tank and outside the tank (top and around) are shown in Figure 7 and Figure 8. The result is that the outside of the shell has a temperature rise of about 34 ÷ 46^{o}C.

The great development of numerical simulation CFD allows us to see the heat transfer and temperature flow in the explosion-proof enclosure; in winding gaps and in core heat radiation as shown in Figure 9.

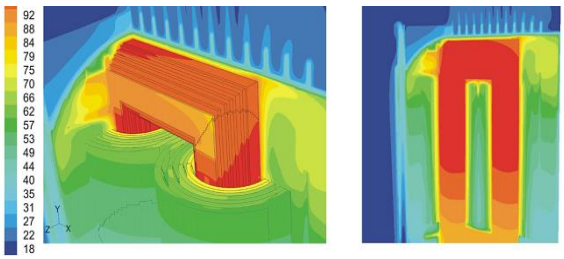

a) *b)*

Figure 9. *Temperature distribution (^{0}C) of tank shell inside in no load; a) Horizontal section between core and windings; b) Vertical section between core and gap*

6.2. Short – circuit

The CFD numerical simulations and Experiments are analyzed in the case of short circuit. The temperature distribution results are shown in Figure 10 and Figure 11.

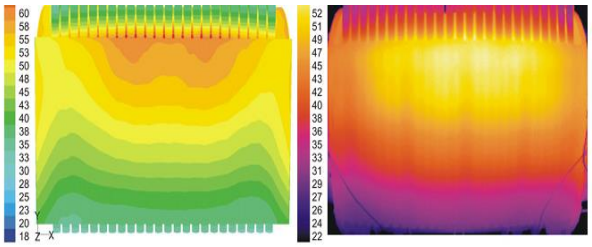

a) *b)*

Figure 10. *Temperature distribution (^{0}C) of tank shell outside in short circuit; a) Numerical simulation CFD b) Experimental measurement*

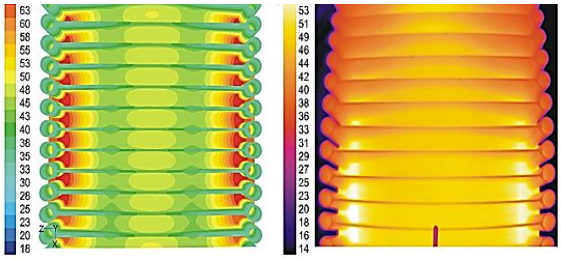

a) *b)*

Figure 11. *Temperature distribution (^{0}C) top of tank shell outside in short circuit; a) Numerical simulation CFD; b) Experimental measurement*

Discussion of results in Short circuit mode:

In the case of a short circuit, the heat source for the windings was determined in the range of q_v = 13.8 ÷ 37.8 Wm^{-3} (Figure 12).

See Figure 12, The great development of numerical simulation CFD allows us to see the heat source from the windings should have a much higher temperature than the other elements. The LV winding is significantly hotter than the HV winding; According to the temperature flow, we see that hot air escapes from the cooling air ducts.

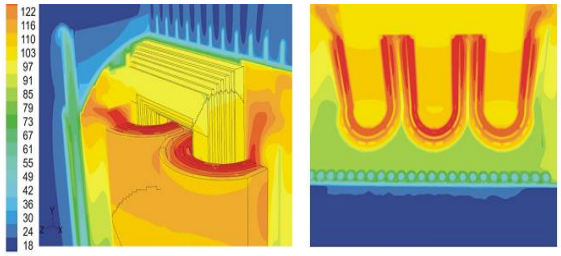

a) *b)*

Figure 12. *Temperature distribution (^{0}C) of tank shell inside in Short circuit; a) Horizontal section between core and windings b) Vertical section between core and gap*

Table 2. *Temperature distribution (^{o}C) at 09 different point*

The points	No-load test			Short - circuit test		
	Measure	CFD	Error (%)	Measure	CFD	Error (%)
1	94	92	2.1	92	99	7.6
2	104	99	4.8	94	98	4.2
3	98	95	3.1	94	99	5.3
4	70	76	8.6	81	80	1.2
5	74	72	2.7	111	114	2.7
6	34	32	5.9	25	22	12
7	21	19	9.5	17	18	5.9
8	35	40	14.3	56	61	8.9
9	29	32	10.3	45	49	8.9

The results obtained from the computations were also compared with data captured during both the CFD simulations and the Experimental model in No load, short circuit, see Table 2. The results show that the accuracy of temperature in the CFD simulations is very close to the Experimental model by outside and inside temperature sensors in nine different locations. In the no-load test, the temperature error in the range (min ÷ max) = (2.1÷14.3)%, In the short-circuit test, the temperature error in the range (1.2÷8.9)%.

Furthermore, numerical simulation CFD shows the results of heat transfer, temperature flow in the explosion chamber; winding clearances and core heat radiation at no-load and short-circuit tests. Also, we also do thermal analysis in rated mode, the result is in Figure 13.

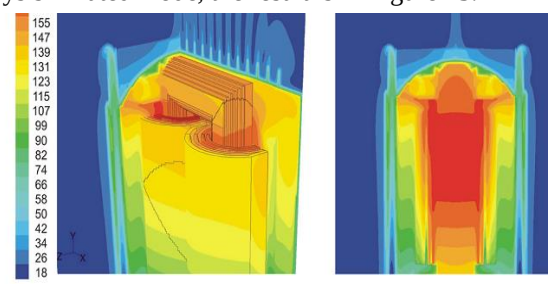

a) *b)*

Figure 13. *Temperature distribution (^{0}C) of tank shell inside in rate current; a) Horizontal section between core and windings b) Vertical section between core and gap*

We continue to analyze and compare in no-load, rated,

and short circuit tests; This extraction is based on the isothermal shapes of the outer tank and the outer tank of the tank with infrared photographs. From there, the hottest spots occur on the tank surfaces, the results are shown in Table 3.

Table 3. *Average and maximum temperature (^{0}C) of transformer in no load, short circuit and rate current*

Results of Temperature (^{0}C)		Test modes		
		No load	Short circuit	Rate current
Average temperature - Experimental measurement	HV winding	38,5	115,7	128,2
	LV winding	51,7	124,9	143,7
Average temperature – CFD model	HV winding	42,8	111,7	132,5
	LV winding	58,9	128,8	161,4
Maximum temperature –CFD model	HV winding	65,7	134,4	135,7
	LV winding	71,5	148,4	169,8

7. Conclusion

In this paper, the temperature mathematical model is developed from the chaotic kinetic energy model and the inside and outside radiant heat transfer to calculate the transformer heat. This mathematical model is applied to the calculation of heat transferring, the temperature rises of an air-cooled dry transformer placed in an explosion-proof enclosure with a capacity of 560kVA - 6/(1.2/0.69)kV.

This study has conducted two parallel models: experimental and numerical simulation CFD. Transformer nine positions are analyzed and compared. The results of the temperature parameter are in the no-load and short-circuit test cases. The result of no-load, the temperature difference is between 0÷ 6^{0}C, the result of short-circuit, the temperature difference is between 0÷ 7^{0}C. At the same time, the average temperature results on the HV and LV windings are analyzed and compared with each other.

The great development of numerical simulation CFD allows us to see the heat transfer and temperature flow in the explosion-proof enclosure; In the winding gaps and in the heat radiation of the steel core. The results of this study found that the hottest spots occurred on the winding or tank surfaces. It is easier to perform the rated mode than the Experimental measurement. We do this by increasing the mesh fineness, we increase the accuracy of the result. Finally, the numerical simulation model CFD has opened up the study of heat transfer models for different electrical equipment and machines.

Acknowledgment: This work was supported by the project B2022-DQN-03 sponsored by the Ministry of Education and Training, Vietnam.

REFERENCES

[1] Pham Van Binh, Le Van Doanh, *Transformer – Theory – Operation – Maintenance and Testing*, Science & Technology, Publishing company Hanoi, 2011.

[2] Vu Gia Hanh, Phan Tu Thu, Tran Khanh Ha, *Electric Machine I*, Science & Technology Publishing company Hanoi, 2009.

[3] M. Xiao and B. X. Du, "Effects of high thermal conductivity on temperature rise of epoxy cast winding for power transformer", *IEEE Transactions on Dielectrics and Electrical Insulation*, Vol. 23, No. 4, 2016, p. 2413–2420.

[4] M. Eslamian, B. Vahidi, and A. Eslamian, "Thermal analysis of castresin dry-type transformers", *Energy Conversion and Management*, Vol. 52, No. 7, 2011, p. 2479–2488.

[5] J. Smolka, D.B. Ingham, L. Elliott, A.J. Nowak, "Enhanced numerical model of performance of an encapsulated three-phase transformer in laboratory environment", *Applied Thermal Engineering*, Vol. 27, No. 1, 2007, p.156–166.

[6] Juan C. Ramos, Maxi. Beiza, Jon Gastelurrutia, Ale. Rivas, RaúlAntón, Gorka S.L, Ivánde Miguel "Numerical modelling of the natural ventilation of underground transformer substations", *Applied Thermal Engineering*, Vol. 51, No. 2, 2013, p.852–863.

[7] JacekSmolka, "CFD-based 3-D optimization of the mutual coil configuration for the effective cooling of an electrical transformer", *Applied Thermal Engineering*, Vol. 50, No. 1, 2013, p.124–133.

[8] Doan Thanh Bao, Doan Duc Tung, Pham Hung Phi, Pham Van Binh, "Calculation of the sum Short Circuit Stress on Windings of Amorphous Core Transformer", *University of Danang - Journal of Science and Technology*, ISSN 1859 -1531, 11(96), No. 2, 2015, p.2-10.

[9] M. A. Arjona, R. B. B. Ovando-Martínez, and C. Hernandez, "Thermal– fluid transient two-dimensional characteristic-based-split finite-element model of a distribution transformer", *IET Electric Power Applications*, Vol. 6, No. 5, 2012, p. 260.

[10] E. Rahimpour and D. Azizian, "Analysis of temperature distribution in cast-resin dry-type transformers", *Electrical Engineering*, Vol. 89, No. 4, 2007, p. 301–309.

[11] K. Preis, O. Biro, I. Ticar, "FEM analysis of eddy current losses in nonlinear laminated cores", *IEEE Transactions on Magnetics*, Vol. 41, No. 5, 2005, p.1412–1415.

[12] Shi Hualin; Xiong Bin; Feng Yun; Li Guohui, "Simulation Analysis of Temperature Distribution of Oil-immersed Self-cooled Transformer under Different Environmental Conditions", International Conference on Electrical Machines and Systems (ICEMS), 2019, doi: 10.1109/ICEMS.2019.8922368.

[13] E. Rahimpour, D. Azizian, "Analysis of temperature distribution in cast-resin dry-type transformers", *Electrical Engineering*, Vol. 89, No. 4, 2007, p. 301–309.

[14] A. Boglietti, A. Cavagnino, D. Staton, M. Shanel, M. Mueller, and C. Mejuto, "Evolution and modern approaches for thermal analysis of electrical machines", *IEEE Transactions on Industrial Electronics*, Vol. 56, No. 3, 2009, p. 871–882.

[15] W. Ning, X. Ding, "Three-Dimensional Finite Element Analysis on Fluid Thermal Field of Dry-Type Transformer", *Instrumentation, Meas. Comput. Commun. Control (IMCCC)*, Second Int. Conf., 2012, p. 516–519.

[16] Y. Chen, C. Zhang, Y. Li, Z. Zhang, W. Ying, and Q. Yang, "Comparison between Thermal-Circuit Model and Finite Element Model for Dry-Type Transformer", *2019 International Conference on Electrical Machines and Systems (ICEMS)*, 2019, doi:10.1109/icems.2019.8922410.

[17] Y. Li, Y. J. Guan, Y. Li, and T. Y. Li, "Calculation of Thermal Performance in Amorphous Core Dry-Type Transformers", *Advanced Materials Research*, Vol. 986–987, 2014, p. 1771–1774.

[18] Smolka, J., & Nowak, A. J, "Experimental validation of the coupled fluid flow, heat transfer and electromagnetic numerical model of the medium-power dry-type electrical transformer", *International Journal of Thermal Sciences*, Vol. 47(10), 2008, 1393–1410

[19] N. Yüksel, *The Review of Some Commonly Used Methods and Techniques to Measure the Thermal Conductivity of Insulation Materials*, in Insulation Materials in Context of Sustainability, 2016, p. 114–136, doi:10.5772/64157.

[20] V. V. S. S. Haritha, T. R. Rao, A. Jain, and M. Ramamoorty, "Thermal modeling of electrical utility transformer", *International Conference on Power Systems*. doi:10.1109/icpws.2009.5442724, 2009, p. 1–6.

[21] D. Zhou, Z. Li, C. Ke, X. Yang, and Z. Hao, "Simulation of transformer windings mechanical characteristics during the external short-circuit fault", Proc. *5th IEEE Int. Conf. Electr. Util. Deregulation, Restruct. Power Technol. DRPT 2016*, p. 1068–1073

[22] Analysis "Ansys Maxwell 3D V.19R1", *User's guide - Maxwell 3D*, Advanced Technology Joint Stock Company, p. 250, 2019.